Supplement 1. Details of the super-individual approach used in the model.

The IBM uses the super-individual approach that enables a fixed number of model individuals to be followed throughout the simulation. Each super-individual represents a number (termed worth) of identical individuals in the population that is set at the time of initiation of the super-individual (Scheffer et al. 1995, Rose et al. 2013, 2015). The same number of super-individuals remain in the population throughout the entire simulation; mortality acts by reducing the worth of each super-individual over time. When a super-individual reaches a maximum age, its information is reset to null conditions and the super-individual becomes available to be initiated to represent young produced in the next year.

All model outputs are expressed by accounting for the worths of the super-individuals. For example, population abundance is the sum of the worths of the super-individuals and averaged values of outputs (e.g., mean size, stage duration) is determined as weighted averages with the worths of each super-individual as the statistical weighting factor.

In the winter flounder IBM, each offspring year-class is represented in the offspring module by 420 super-individuals, with their initial worths based on the total number of ova produced for that year. When the super-individuals exit the offspring module as recruits, they are randomly sampled (with replacement) to populate the 30 super-individuals used to represent them as new age-1 super-individuals in the parent module. The worths of the selected 30 super-individuals are adjusted proportionally, until their sum (after adjustment) equals the total worth of all (up to 420) offspring super-individuals at recruitment. The super individuals from a single year-class are then followed by age class from years 1 to 14. All super individuals are removed at age 15, which is the oldest age observed in a stock assessment (NEFSC 2011). We use 420 super-individuals in the offspring module so there is a super-individual to represent the young from the maximum of 30 super-individuals per age-class times 14 age-classes in the adult module that could potentially spawn. Using 30 super-individuals per year-class is sufficient to generate convergent results (we repeated the spin-up and reference simulation with 60 super-individuals per age-class and obtained very similar model output). In addition, when decades were repeated, predicted SSB showed almost identical behavior every decade (main document Fig. 8); following too few super-individuals would have generated differences among the repeated decades.

Supplement 2. Calibration of Reference simulation

We first describe the laboratory and field data used to specify processes and estimate parameter values for their formulations (sections 1-5). We then show simulation results that confirmed the realism of larval and juvenile growth (section 6), and the model adjustments needed to ensure the Reference simulation generated a spawner-recruit relationship that was consistent with some of the major general features of the observed spawner-recruit relationship used in the recent stock assessment (section 7).

S2.1. Reproduction

S2.1.1. Oocytes and ova (equations 1, 4, 10; parameters a_s, Q_s, a_o, b_o, a_r, b_r*)*

A statistical analysis of water temperature data from the Mid-Atlantic and Northeast biogeographic regions of the NOAA National Estuarine Research Reserve System (2017) was performed to parameterize oocyte and ova stage development. The target was to be able to predict the latitudinal patterns in timing of winter flounder spawning (Klein-MacPhee 1978, DeCelles & Cadrin 2011). A sinusoidal model of temperature was fit to each of 55 locations from Virginia to Maine and the parameters a_s and Q_s were adjusted to project spawning timing across this range. This approach assumes that the onset of oocyte vitellogenesis is similar across latitudes and that estuarine and coastal shelf temperatures are sufficiently correlated so that estuarine temperatures can be used predict spawning without explicitly modeling complex seasonal migrations. Press et al. (2014) showed that the onset of ovarian development was essentially synchronized across all three US winter flounder stocks, with a minimum gonad size in July and a noticeable increase by October. We used August 21 as an estimate for the average onset of oocyte vitellogenesis across US (Press et al. 2014) and Canadian (Dunn & Tyler 1969, Burton & Idler 1984) stocks. Using the time series of temperatures, simulated spawning start and ending was predicted to be January 6 to March 8 in the southernmost location (Chesapeake Bay, Virginia; station “cbvcbwq”) and April 14 to June 1in the northernmost location (Webhannet River, Maine, station “welhtwq”).

The four parameters (a_o, b_o, a_r, b_r) governing ovum mass were based on our reanalysis of data from Buckley et al. (1991b), main document Table 1). In their dataset, mass of strip-spawned, hydrated ova decreased by about 20% over the course of the spawning season (70 d, starting on February 1) and increased by about 20% across the range of maternal lengths (260-396 mm). Representing the initial mass of an individual ova (at spawning season onset) as a linear function of adult length and the subsequent decrease in mass as the spawning season proceeds as an exponential decay (b_r=0) due to respiration (see Figure S6 for comparison to embryos and later stages) provided a good fit to the data, and explained 66% of variability in embryo mass at strip-spawning (1 outlier removed).

S2.1.2. Fecundity and probability of spawning (equations 2–3; parameters a_f, b_f*)*

Potential annual fecundity was parameterized (a_f, b_f) using a back-transformed log-log regression on spawner length from McElroy et al. (2013). Winter flounder have determinate fecundity (Dunn & Tyler 1969, Burton & Idler 1984, McElroy et al. 2013), thus lending themselves to the simplifying assumption used in the IBM of one release of eggs per season per super-individual. The probability of spawning (P) by female size was estimated according to McBride et al. (2013), who reported mean lengths of Southern New England and Mid-Atlantic samples, and assumes that females below 200 mm total length are sexually immature, those above 390 mm are mature, and 50% maturity is reached at about 293 mm. Probability of spawning is represented based on parent length (interpolated with a growth rate to day of spawning), assuming a triangular distribution of the parent length at sexual maturity with minimum a_p=200, maximum b_p=390, and mode c_p=291 (Figure S1). This gives the asymmetrical sigmoidal function for the probability of spawning:

$$P = \begin{cases} 0, & L \le a_p \\ \dfrac{(L - a_p)^2}{(b_p - a_p)\bullet(c_p - a_p)}, & a_p < L \le c_p \\ 1 - \dfrac{(b_p - L)^2}{(b_p - a_p)\bullet(b_p - c_p)}, & c_p < L < b_p \\ 1, & L \ge b_p \end{cases} \qquad \text{(S1)}$$

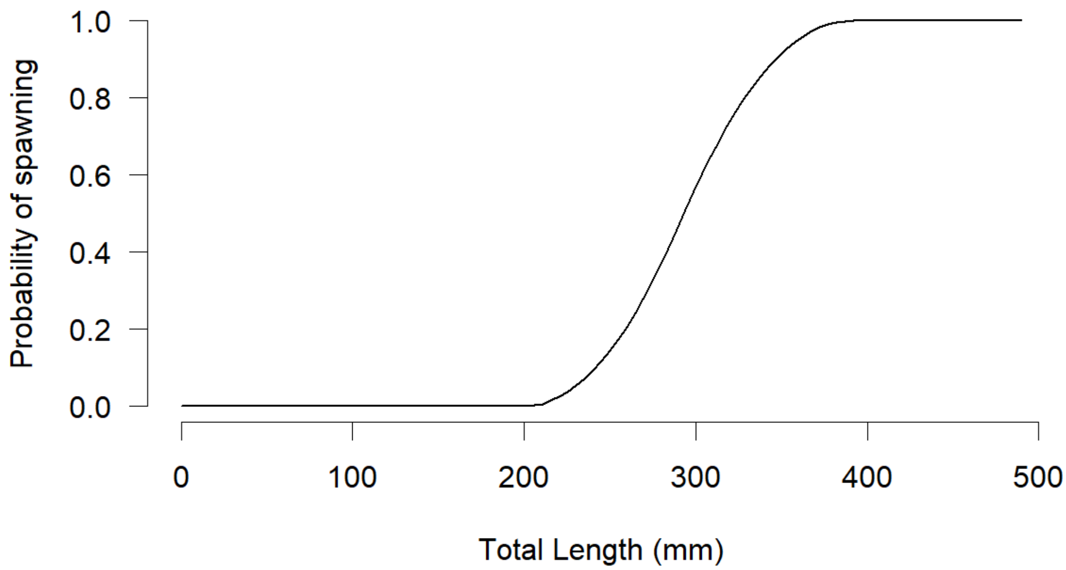

Figure S1. Modeled probability of spawning as a function of length, based on McBride et al. (2013).

S2.1.3. Fertilization and hatching (equations 5–7; parameters a_v, b_v, γ, a_h, b_h)

Fertilization success at a reference temperature of 5 °C in the absence of CO_2 effects was set to 80% by adjusting a_v (fertilization success at 0 °C, equation 5). This is at the low end of mean values reported for artificial fertilization in laboratory studies. For example, fertilization success has been reported as 80-99% (Black et al., 1988), 75-98% (Buckley et al. 1990), 79-93% (Buckley et al. 1991a), and 78-99% (Nelson et al. 1991). There is some evidence for fertilization being less successful *in situ*. In epibenthic net samples of the New York/New Jersey Harbor, from <1% to 75% (median: 40%) of winter flounder eggs collected per year were unfertilized or non-viable for other reasons (Wilber et al. 2013). In Atlantic herring (*Clupea harengus*), which also spawns benthic and adhesive eggs, 9-45% of *in situ* eggs were non-viable as estimated by diver surveys of a Baltic estuarine lagoon (Kanstinger et al. 2018).

The slope of the effect of temperature on fertilization (equation 5) was parameterized using unpublished data on southern New England/Mid-Atlantic (SNE/MA) winter flounder from experiments at the Howard Marine Sciences Laboratory (Figure S2). The same data and analysis were also used to specify CO_2 effects on fertilization (see Supplement 3). To extrapolate from the experiments, which were conducted under a range of different CO_2 treatments and potentially sperm-limited conditions (15% to 52% fertilization success), we focused our analysis on changes in the odds of fertilization (i.e., the ratio of fertilized to unfertilized ova). Across all CO_2 treatments, the odds of fertilization were approximately twice as high at 4 °C than at 13 °C. A generalized additive model (GAM) of the log-odds of fertilization (logit regression) as a function of temperature and smoothed CO_2 provided a good fit to the data (R^2=0.85). Parameter values of a_v and b_v were calculated by back-transforming GAM output from log-odds to raw fertilization success and then fitting linear approximations to the resulting curves ($R^2$0.99).

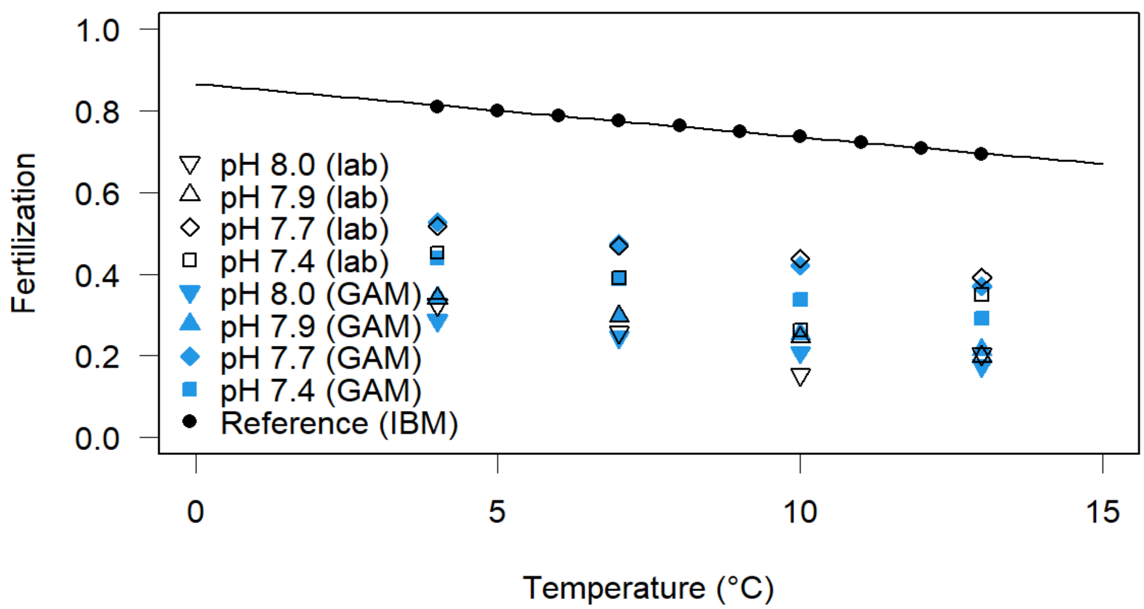

Figure S2. Fertilization success as a function of temperature and pH/CO_2.Lab: unpublished experimental data on fertilization trials under sperm-limited conditions; GAM: back-transformed output of logit regression model fit to lab data and used to parameterize the IBM for field conditions; IBM: offspring model parameterizations. See Supplement 3 for additional details.

Hatching survival of embryos (equation 7) was parameterized (Figure S3) based on a reanalysis of experimental data from Rogers (1976) for 3-14 °C temperature and 10-30 salinity treatments. A GAM was fit to the proportion of hatched and viable larvae as a function of smoothed temperature and salinity (R^2=0.7). The model intercept and slope of the (approximately linear) partial additive temperature effect were used to define a_h=83.14% and b_h=-2.567% °C^{-1}, respectively. Since only the temperature dependency component was used in the IBM, average salinity conditions were used for the data analysis.

The fraction of ova dry mass retained after the chorion is lost at hatching (γ = 49%) was determined by re-analysis of measurements reported in Cetta & Capuzzo (1982). Specifically, we used the ratio of yolk-sac larva dry mass on the day after hatching to embryo dry mass extrapolated to the same day (assuming exponential mass loss, see respiration section) as the fraction of mass lost.

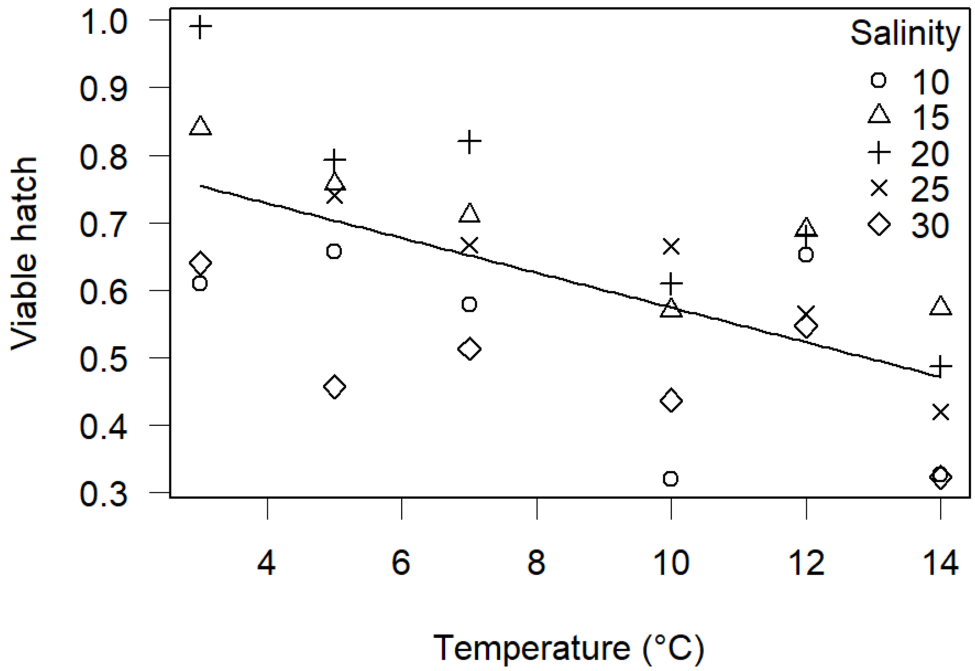

Figure S3. Hatching survival as a function of temperature and salinity. Symbols show lab data from Rogers (1976); line shows model parameterization.

S2.2. Embryo and yolk-sac stage development (equation 1, parameters a_s and Q_s)

We fit a_s and Q_s to mimic embryo and yolk-sac larva stage durations (the inverse of developmental rate) reported in the literature (Figures S4 and S5). The temperature scaling of daily embryo development was parameterized using a back-transformed log-linear regression of median time from fertilization to hatching on temperature reported by Williams (1975). This relationship, originally proposed for 0 to 10 °C, it is quite consistent with data outside this temperature range (Williams 1975) and with many other studies (Rogers 1976, Buckley 1980, 1982, Cetta & Capuzzo 1982, Klein-Macphee et al. 1984, Buckley et al. 1990, Jearld et al. 1993, Keller & Klein-MacPhee 2000).

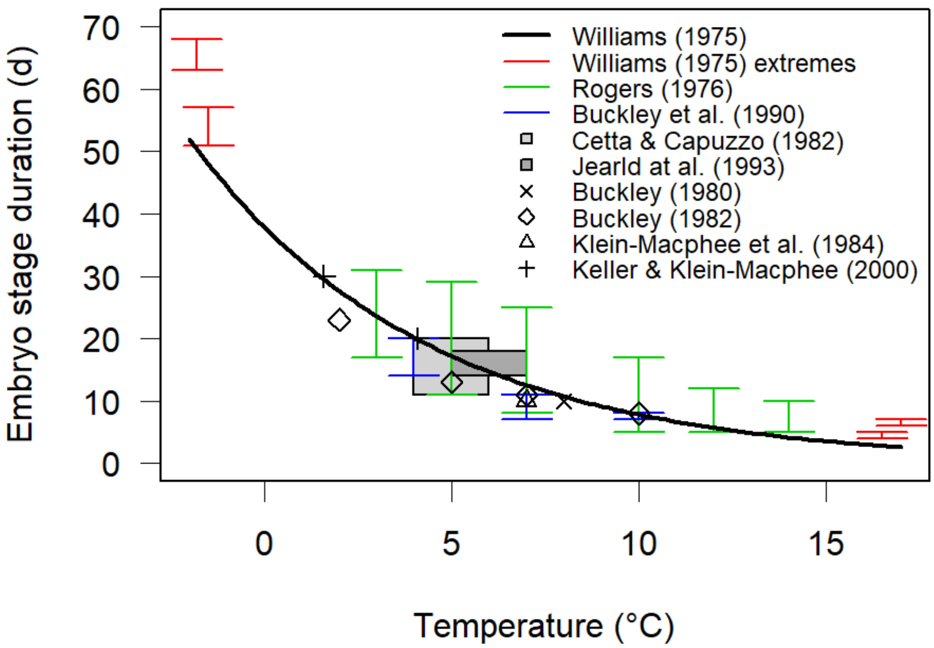

Figure S4. Embryo stage duration as a function of temperature. The IBM used the published fit from Williams 1975 (black line). Boxes show data when reported as ranges.

Temperature scaling of daily yolk-sac larva development was based on a dataset for the duration from hatching to first-feeding at incubation temperatures of 4, 7, and 10 °C (Buckley et al. 1990). Here, a_o was set to the inverse of the mean duration at 10 °C, and Q_s=3.2 was estimated by a nonlinear regression (R^2=0.68, n=18). Measurements from other laboratory studies with smaller temperature ranges (Buckley 1980, 1982, Jearld et al. 1993) are similar to those from Buckley et al. (1990).

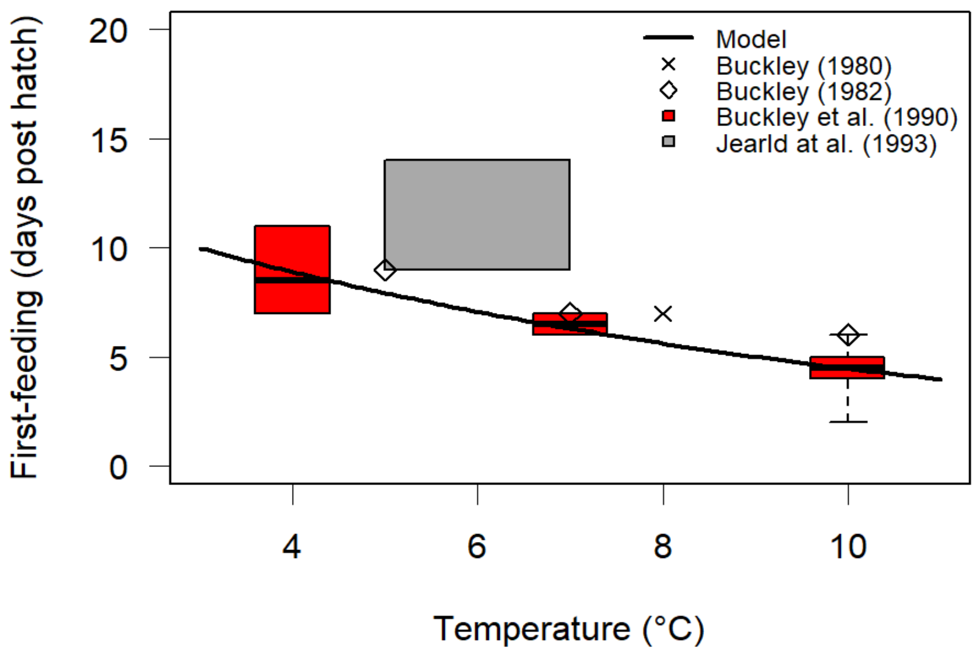

Figure S5. Yolk-sac larva stage duration as a function of temperature. The IBM (line) uses the medians in Buckley et al. (1990). Boxes show data when reported as ranges.

S2.3. Bioenergetics of feeding larvae and juveniles

S2.3.1. Respiration (Equations 8, 10; parameters a_r, b_r, Q_r*)*

Respiration parameters were based on oxygen (O_2) consumption rates of winter flounder eggs (Cetta & Capuzzo 1982), yolk-sac larvae (Cetta & Capuzzo 1982), feeding larvae (Laurence 1975, Cetta & Capuzzo 1982), and juveniles (Voyer & Morrison 1971, Frame 1973a, Laurence 1975). In addition, we used reported dry mass or protein mass loss rates of eggs (Cetta & Capuzzo 1982), yolk-sac larvae (Buckley 1980, 1982, Cetta & Capuzzo 1982, Buckley et al. 1990), and unfed feeding larvae (Buckley 1980), as well as changes in dry mass of strip spawned, hydrated ova (Buckley et al. 1991b). Overall, size-corrected respiration rates increased dramatically from ova to embryos to yolk-sac larvae to inactive feeding larvae to active feeding larvae (Figure S6). Juvenile rates were similar to inactive feeding larval rates, with much lower levels of activity after metamorphosis (Laurence 1975). For yolk-sac and feeding larvae, respiration was substantially faster during respirometry experiments (approximated by oxycalorific equivalent) when they exhibited a “three-fold difference” in O_2 consumption with changes in activity (Cetta & Capuzzo 1982) than during routine activity in rearing tanks (estimated by changes in mean mass from day to day). For yolk-sac larvae and eggs, the respiration rates estimated by O_2 consumption were higher than those based on mass loss.

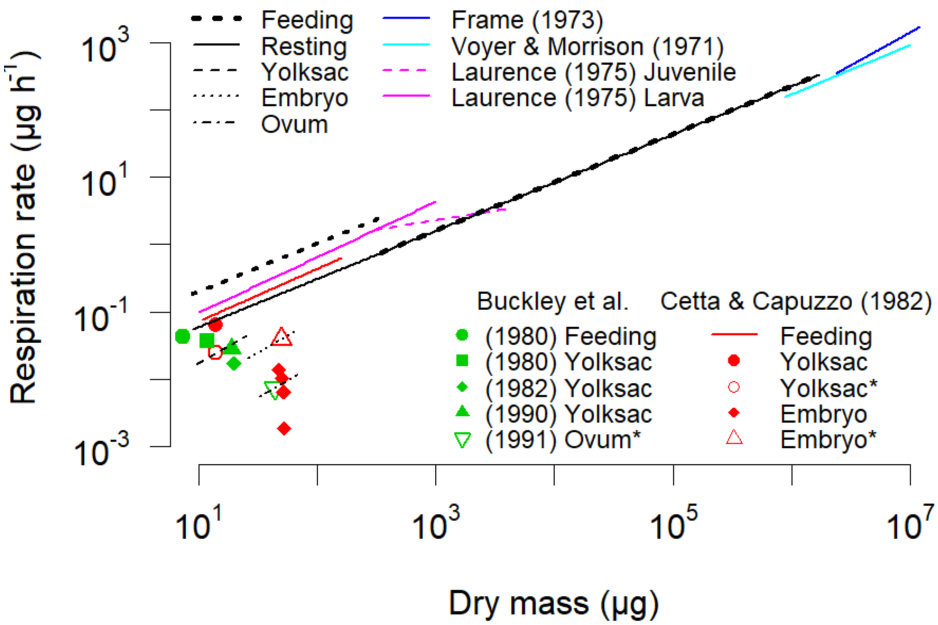

Figure S6. Respiration rate (µg/h) versus dry mass by size and stage at 7 °C (in three cases, extrapolated to 7 °C). Black: model; *: based on dry mass loss; Buckley (1980, 1982) and Buckley et al. (1990): based on protein mass loss; other literature values: based on oxygen consumption.

For feeding larvae and juveniles, over 98% of variability in log transformed O_2 consumption rate was explained by a fitted model with shared length exponent b_r and temperature effect Q_r, but different length-based coefficients a_r for the more active foraging larvae versus more passive juveniles. The shared $Q_r = 2.781$, reflecting a temperature range from 2 to 25 °C, was used for feeding larvae and juveniles. The back-transformed and bias-corrected (Duan, 1983) juvenile value of a_r was used for routine (inactive) respiration of feeding larvae and juveniles. For yolk-sac larvae and eggs, a_r was approximated by exponential mass decline rates fit to data from Cetta and Capuzzo (1982). Different activity parameters (α) for feeding larvae and for juveniles were defined in the process of tuning consumption to match observed growth rates.

S2.3.2. Body shape (parameters a_b, b_b,*)*

We used an allometric length-mass relationship to describe changes in body shape, total length, and dry mass of feeding larvae and YOY juveniles (Figure S7). Parameters a_b and b_b were defined by fitting a power function to two data points representing the respective medians of four wild-caught larvae (Buckley 1981) and eleven juveniles (Frame 1973a). Standard length (SL) (Buckley 1981) was converted to total length (TL) assuming TL = -0.2 + 1.212 x SL (Millstone Environmental Laboratory 2017) and wet mass (Frame 1973a) was converted to dry mass assuming a tissue water content of 79% (Frame 1973b). The derived relationship is consistent with other published field data (Black et al. 1988, Wigley et al. 2003) and measurements from larvae reared in the laboratory (Laurence 1979).

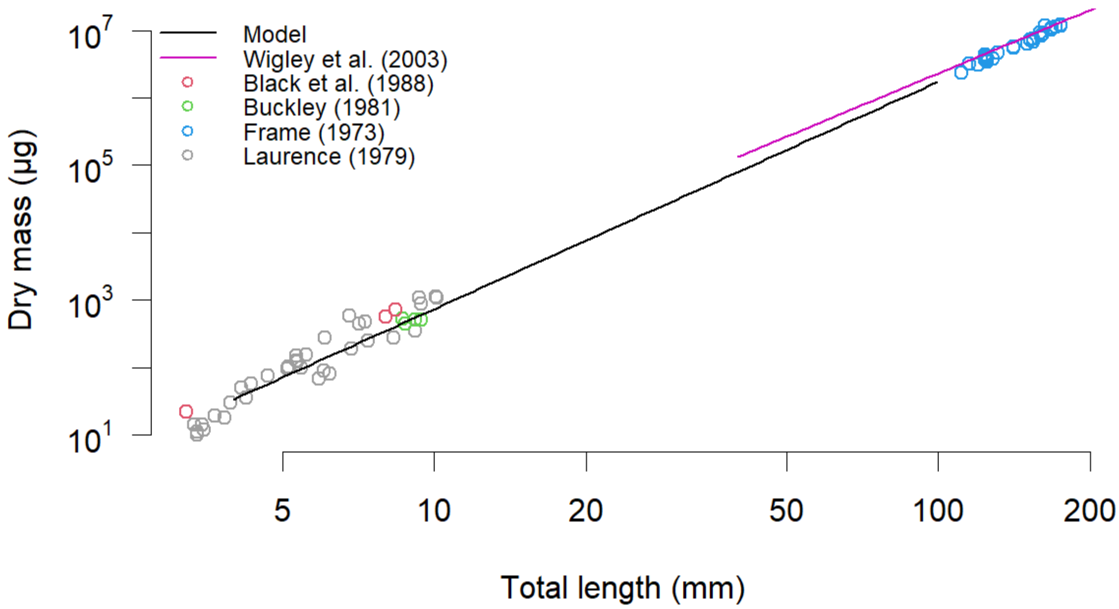

Figure S7. Mass versus length relationships for feeding larvae and juveniles. The transition from larval to juvenile life-stage (i.e., metamorphosis) occurs at ~ 8 mm total length (TL). Dry mass converted from wet mass following Frame (1973b) and TL from standard length following Millstone Environmental Laboratory (2017), where necessary.

S2.3.3. Consumption and digestion (equations 11–14; parameters a_d, b_d, Q_d, a_g, b_g, a_c, b_c, t1, t2, t3, t4, k1, k2, k3, k4*)*

Size-dependent gut content capacities were estimated from published gut and stomach content measurements for winter flounder (Figure S8) among larvae fed high concentrations of nauplii for 12 h (Laurence 1977), and large juveniles to adults fed to satiation on squid (Huebner & Langton 1982). The parameters a_g and b_g were defined using a back-transformed and bias-corrected (Duan 1983) log-log regression of the gut-mass to body-mass ratio on length. For the regression, size was converted from mass to length using the relationship described in 3.B, and assuming 79% water content (Frame 1973b) of large juveniles and adults. The realized level of gut/stomach fullness was generally far below 100% capacity, as apparent in the large range of gut/stomach fullness and demonstrated by direct measurement of maximum capacity (Huebner & Langton 1982).

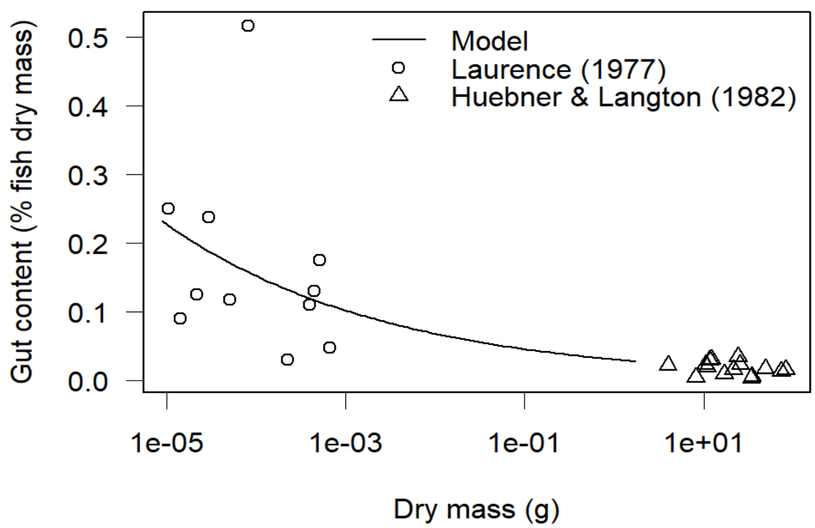

Figure S8. Gut content versus mass for feeding winter flounder larvae and juveniles.

Size-dependent digestion rates were estimated from gut evacuation rates for feeding larvae (Laurence 1977) and for juveniles and adults (Huebner & Langton 1982), assuming a temperature scaling Q_{10} (Q_d) of 2.5 (Figure S9). This same Q_{10} value was used in a generic model of larval fish growth (Huebert & Peck 2014), and is consistent with estimates previously used for juvenile and adult winter flounder (Worobec 1984). Parameters a_d and b_d were defined from a back-transformed log-log regression of evacuation time on length. For the regression, evacuation time was set to the 10 °C temperature-corrected estimates reported by Laurence (1977) at 4 and 8 mm length (the for feeding larvae in the IBM) and reported by Huebner & Langton (1982) at 127.8 and 313.7 mm (approximating the size range in their study).

The estimate of digestive efficiency (β = 0.675) was taken from a generic model of larval fish growth (Huebert & Peck 2014), and lies between the ~60% total assimilation efficiency and ~80% organic assimilation efficiency of summer flounder juveniles (Malloy & Targett 1991, 1994).

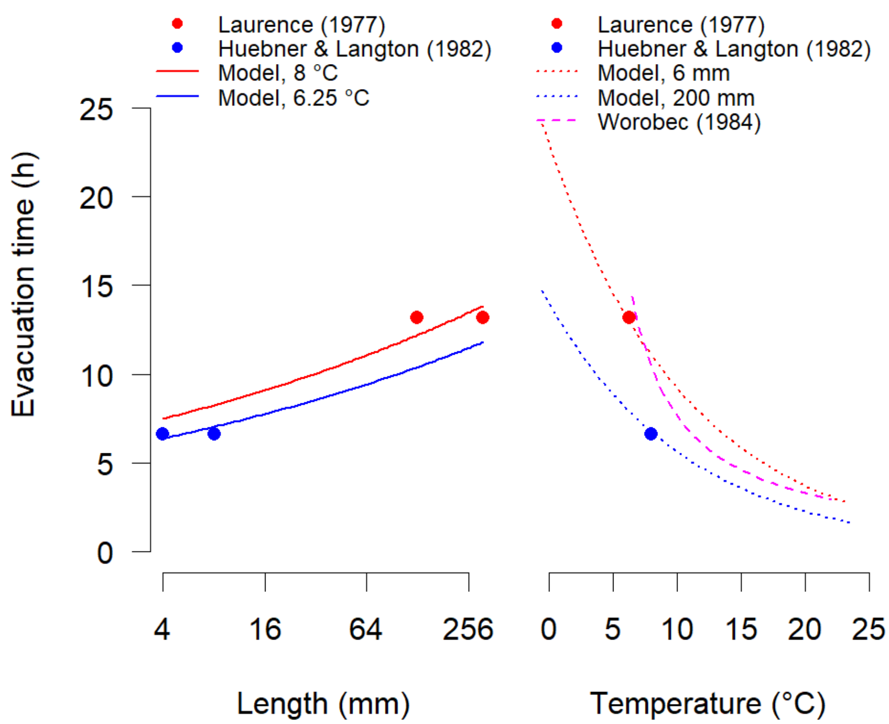

Figure S9. Gut evacuation time versus length (left panel) and temperature (right panel). Model output is shown for temperatures and lengths corresponding to published studies (Laurence 1977, Huebner & Langton 1982).

Consumption was partially tuned by specifying the parameters of the temperature-dependent function $f(T)$ to minimize the error between observed and modeled growth rates of SNA/MA winter flounder larvae at temperatures from 2 to 12 °C (Laurence 1975, Buckley 1982, Keller & Klein-MacPhee 2000) and juveniles from 17 to 26 °C (Sogard 1992, Meng et al. 2000). Of the six parameters of $f(T)$, $t1$=0 and $t4$=30 were based on thermal tolerance studies synthesized by Klein-MacPhee (1978), and $t2$=14 and $t3$=18 were estimated from juvenile consumption measured in laboratory experiments (Frame 1973b). Near-maximum consumption was set to $k2$=$k3$=0.98, following Thornton and Lessem (1978). The remaining parameters $k1$ and $k4$ were tuned simultaneously with a_c and b_c (allometric scaling of consumption) and with activity α of foraging larvae and juveniles to obtain realistic growth (section 6).

S2.4. Mortality (equations 15–17; parameters b_m, Q_m)

Mortality of feeding larvae and juveniles was tuned to approximate the SNE/MA stock-recruit relationship (NEFSC 2011) and also to be consistent with estimates of size effects and temperature effects on mortality. We report on the length and temperature dependencies of mortality rate here and also as part of the description of the fitting to the spawner-recruit relationship (section 7).

The length-specific mortality rates of estuarine and shelf larvae in general (Houde and Zastrow, 1993), as well as winter flounder larvae (Pearcy 1962, Keller & Klein-MacPhee 2000, Millstone Environmental Laboratory 2017) and juveniles (Pearcy 1962, DeLong et al. 2001), suggest $b_m \cong -1$ which was the parameter value used here (Figure S10). This falls within one standard error of the mean mortality rate of -0.77 (±0.28) estimated by DeLong et al. (2001) for June 1988 to October 1999 based on juvenile winter flounder length-frequency distributions in Narragansett Bay.

Size-specific mortality of embryos and yolk-sac larvae was fixed at the same level as for feeding larvae of their initial length (4 mm), because these stages undergo changes in size that are ambiguous, i.e., higher (but decreasing) mass and lower (but increasing) length relative to initial feeding larvae.

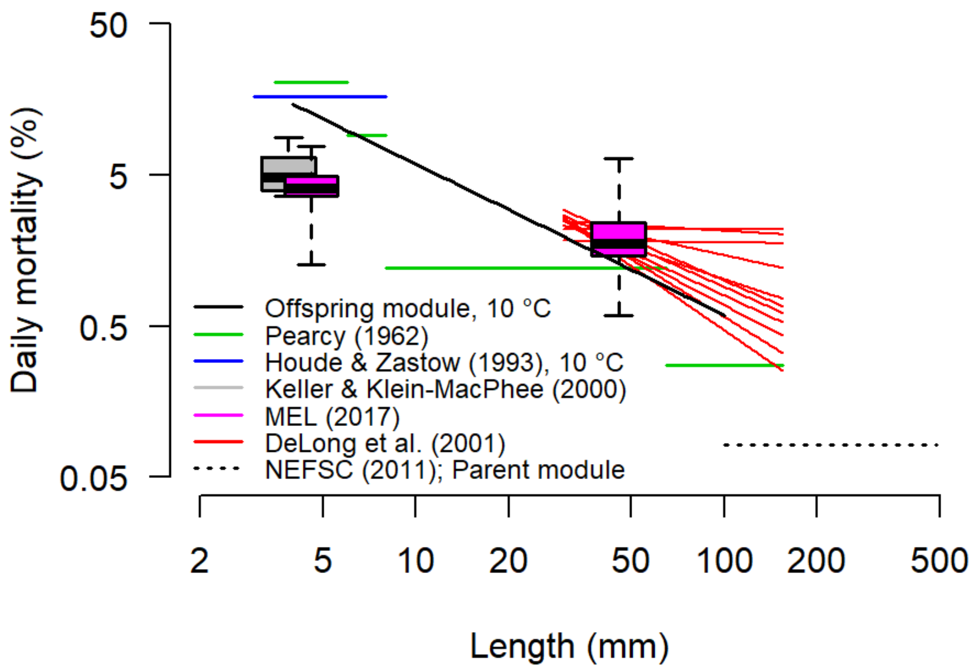

Figure S10. Daily mortality versus length. All estimates except for Houde & Zastrow (1993, shown for 3 to 8 mm) are specific to SNE/MA winter flounder with no temperature correction and thus are likely biased high for larvae (cooler waters) and low for YOY juveniles (warmer waters). The offspring module relationship does not include density-dependent juvenile mortality. The transition to the parent module occurs on December 31 irrespective of length (for context, 86 mm was the typical length of recruits in IBM simulations).

There is substantial evidence that mortality rates of winter flounder eggs (Keller & Klein-MacPhee 2000, Taylor & Danila 2005), larvae (Keller & Klein-MacPhee 2000), and juveniles (DeLong et al. 2001, Taylor 2003, Manderson et al. 2006, Millstone Environmental Laboratory 2017) tend to increase with temperature, which is usually attributed to greater consumption by predators. Empirical estimates for a mortality-related Q_{10} temperature relationship in fish include 1.9 (Brown et al. 2004) and 2.2 (McCoy & Gillooly 2008) for adults (both calculated for 15 °C), 2.2 (Pepin 1991) for feeding (pelagic) larvae, and 2.0 (Houde & Zastrow 1993) for pelagic larvae of estuarine and continental shelf taxa (our re-analysis of their Figure 2A). Similarly, the secondary production of estuarine benthic invertebrates (predators of winter flounder eggs and juveniles) is characterized by Q_{10} values between 2 and 2.5 (Tumbiolo & Downing 1994), and maintenance of cohort production (growth versus mortality) requires equivalent increases in consumption (Taylor 2003, Taylor & Danila 2005). The overlap of spatial distributions of winter flounder eggs (Taylor & Danila 2005) and juveniles (Manderson et al. 2006) with some of their major predators also tends to increase with temperature. Some time series of juvenile winter flounder distributions suggest much larger temperature effects on mortality (DeLong et al. 2001, Millstone Environmental Laboratory 2017), but estimates of mortality in the field may be confounded by emigration from the sampled area. To avoid over-emphasizing the negative effects of the historical warming encapsulated within model simulations we used a conservative value (Q_m = 2.0) for all stages from embryos to YOY juveniles.

S2.5. Parent module growth and survival (equations 18–20; parameters L_∞, k_v, A_v, m_n, m_f, i, $L_{50\%}$)

Parameters for growth and mortality of large juveniles (after recruitment at ~86 mm TL) and adults in the parent module were based on the SNE/MA winter flounder population (main document Table 2). We used von Bertalanffy age-length relationship parameters for females age 2 to 8 from south of Cape Cod (Witherell & Burnett 1993). Annual natural mortality rate, m_n, for these ages was estimated at 0.3 yr^{-1} and annual fishing mortality rate, m_f, for maximum sustainable yield was estimated as 0.29 for the SNA/MA population (NEFSC 2011). Increasing susceptibility to fishing with fish length was parameterized using age-based estimates (NEFSC, 2011) converted using the above age-length relationship (Witherell & Burnett 1993). Estimates for two different blocks of time (1981-1993 and 1994-2010) were equally weighted, and i and $L_{50\%}$ were fit by non-linear regression (equation 20).

S2.6. Check on larval and juvenile growth

To evaluate model performance with respect to bioenergetics, we simulated growth under conditions that roughly mimicked laboratory and field conditions for various published studies of SNE/MA winter flounder (Figure S11). Besides the data used for model tuning (Laurence 1975, Buckley 1982, Sogard 1992, Keller & Klein-MacPhee 2000, Meng et al. 2000), we included additional studies for yolk-sac larvae (Buckley 1980, Cetta & Capuzzo 1982), feeding larvae (Cetta & Capuzzo 1982, Jearld et al. 1993, Millstone Environmental Laboratory 2017), and juveniles (Pearcy 1962, Mulkana 1966, Stierhoff et al. 2006). We used reported values or estimates of temperatures, day-lengths, starting and ending conditions (larval stage and size), and durations representative of the published conditions. When necessary, individual dry mass was inferred from other measurements (e.g., length, protein mass). Overall, the observed and predicted growth rates were highly correlated (R^2=82%, 61 data points from 12 studies) and the data scatter matched the 1:1 identity line reasonably well (R^2=50%, sum of squares method) (Figure S11).

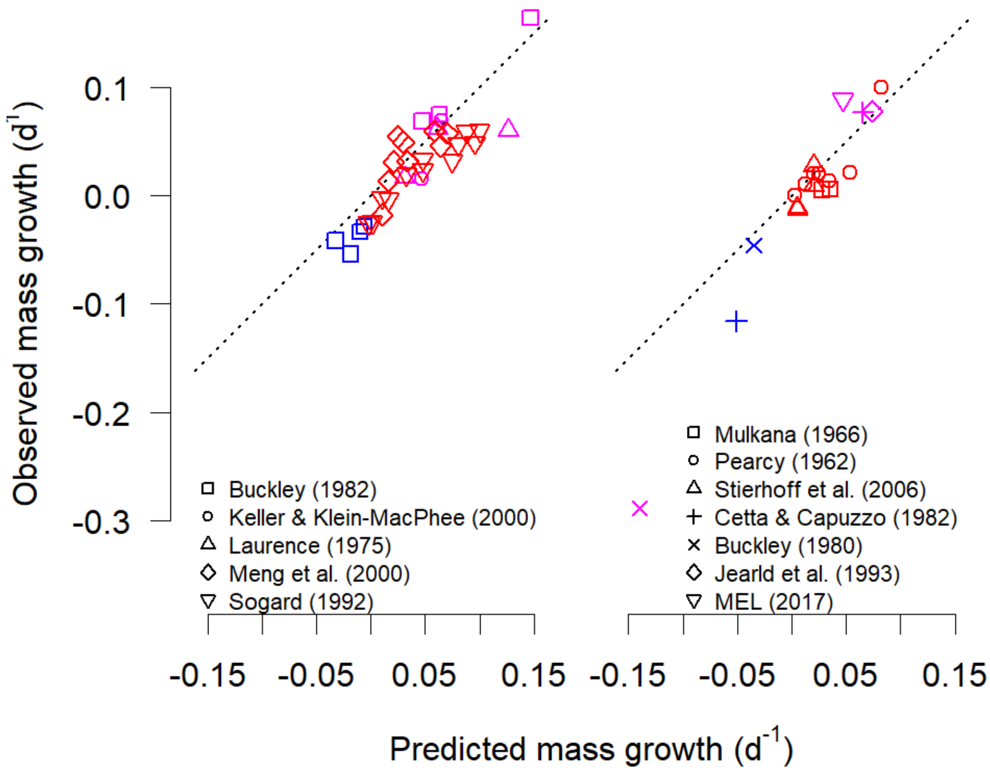

Figure S11. Empirically observed versus model predicted growth rates (daily relative growth in dry mass) in 12 studies of SNE/MA winter flounder yolk-sac larvae (blue), foraging larvae (purple) and juveniles (red). Left panel: studies used to tune the parameterization of the model; right panel: additional studies. Accurate predictions should fall near the dashed 1:1 identity line.

To evaluate whether the magnitude and time course of growth among modeled feeding larvae and YOY juveniles was appropriate for the SNE/MA winter flounder population, the output from the Reference simulation was compared to published field data from New Jersey (Sogard 1992), Connecticut (Pearcy 1962, Millstone Environmental Laboratory 2017), and Rhode Island (Mulkana 1966) (Figure S12). In all cases, the mean sizes observed in the field overlapped with the range of lengths in the simulation with no evidence of bias for any particular time of year.

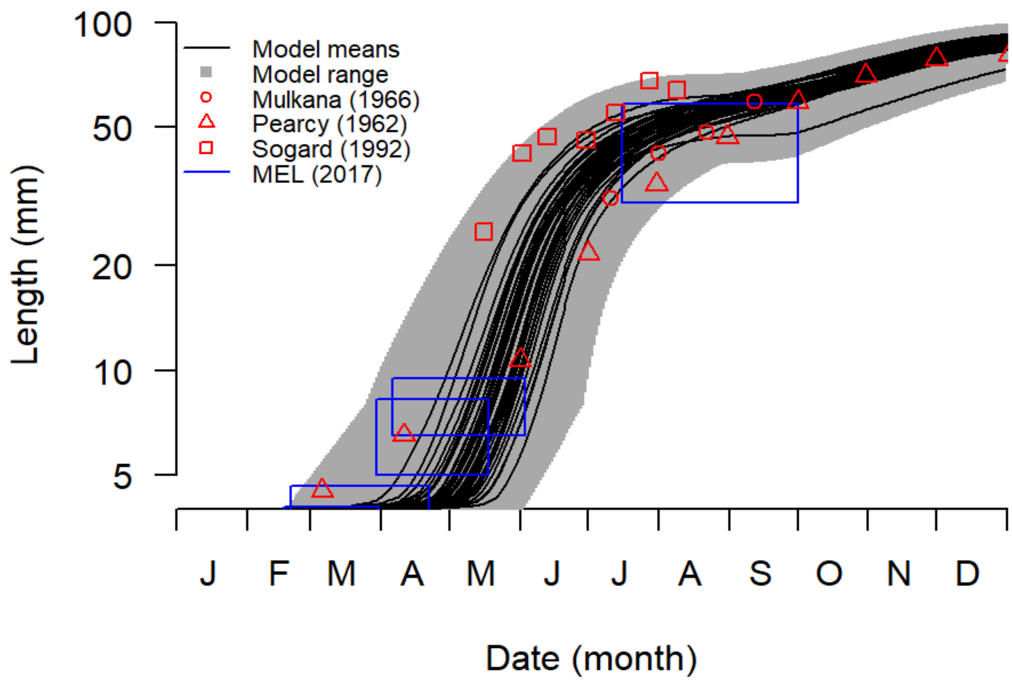

Figure S12. Comparison of mean lengths of feeding larvae and juveniles (pooled) in the 1977-2016 Reference simulation with empirical data. Boxes from MEL (2017) are reported ranges of values.

S2.7. Spawner-recruit calibration (equations 16–17, parameters a_m, d_m)

Mortality of feeding larvae and juveniles was tuned to approximate the SNE/MA stock-recruit relationship (NEFSC, 2011) and also to be consistent with estimates of size and temperature effects on mortality (section 4). The parameters a_m and d_m (for density-independent and density-dependent mortality) were tuned (adjusted) until the model generated a stock-recruit relationship (Figure S13) with a steepness estimate of about 0.61 (NEFSC, 2011). To better match the recruitment observed in field surveys, we used an alternative measure of recruitment from the IBM simulation. We used the number of age-1 individuals entering the parent module in August 20, which is ~83% of recruitment to December 31 used with the Reference and other simulations (natural mortality for the period from December 31 to August 20 was calculated as in the parent module). Similar to the Recovery experiment, this involved generating an unfished Reference-conditions population for which 14 years of fixed recruitment of 71.58 million age-1 (~102 mm TL) individuals was assumed, which is the maximum historical recruitment estimate (NEFSC, 2011). The parameters a_m and d_m were then adjusted until the mean simulated recruitment for the period considered in the 2011 stock assessment (1981-2010) was 71.58 million individuals for the unfished Reference conditions population and 61% of this level for a population with identical age structure as the unfished population but only 20% of the biomass (i.e., matching a steepness target of 0.61 times the maximum recruitment at 20% of virgin stock biomass). The resulting range of z was consistent with the reported range (Pearcy 1962, Houde & Zastrow 1993, Keller & Klein-MacPhee 2000, DeLong et al. 2001, Millstone Environmental Laboratory 2017).

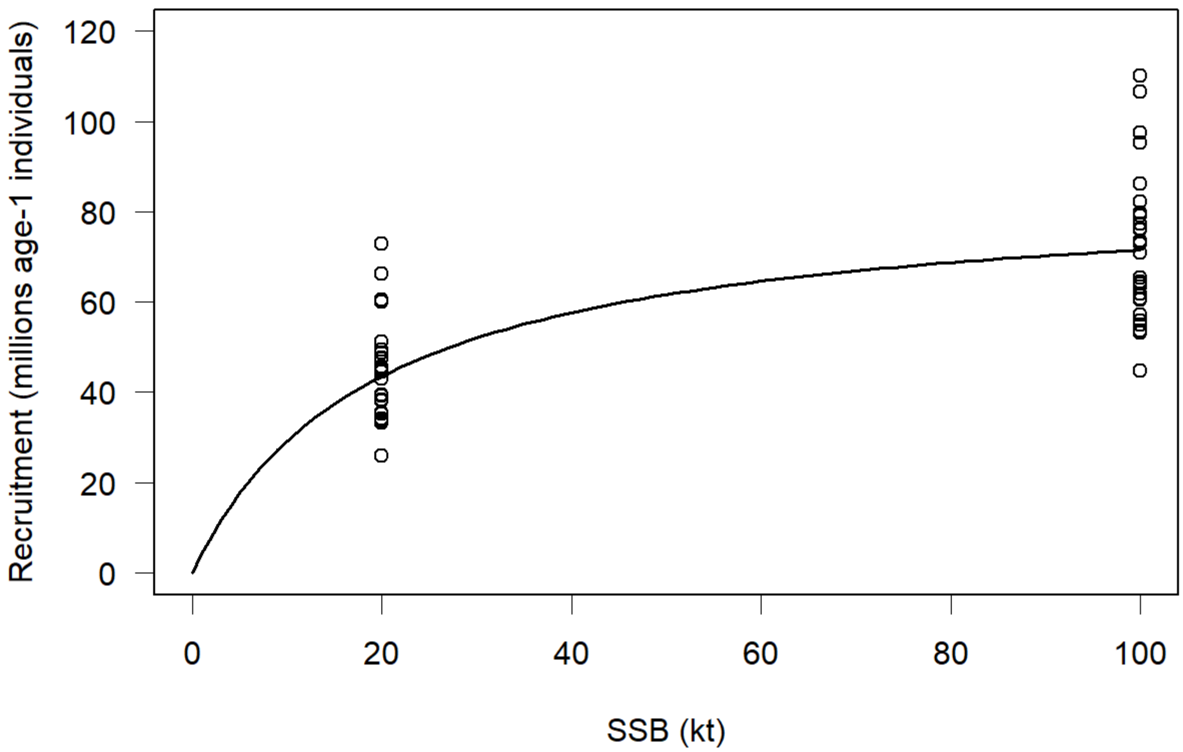

Figure S13. Stock-recruit relationship showing the final results after tuning the density-independent and density-dependent components of juvenile mortality (parameters a_m and d_m in equations 16-17) to obtain a relationship similar to that reported in NEFSC (2011). Recruitment for 1981-2010 (circles) was generated by short IBM runs (spawning to recruitment) starting with a fixed SSB (unfished and 20% of unfished SSB) and using daily temperatures for each year. Unfished SSB was estimated as 99.92 kt. Average 1981-2010 recruitment matched the target value of recruitment at unfished SSB of 71.58 x 10^6 age-1 individuals and the target steepness value of 0.61.

Supplement 3. Estimates for elevated CO_2 effects.

Two sources of information were used to specify effects of elevated CO_2 and OA scenarios for the model: data from experiments on winter flounder early life stages performed at the NOAA Howard Marine Sciences Laboratory (unpublished data, Table S1) and data from published sources on other fish species (see main document Table 3).

The NOAA data were drawn from three experiments on effects of elevated CO_2 on winter flounder. The experiments were designed for examining the effects of multiple environmental factors on multiple response variables. The three experiments assessed the effects of CO_2 and temperature on fertilization rate (Experiment 1), size at metamorphosis (Experiment 2), and consumption rates of juveniles shortly after metamorphosis (Experiment 3). Metamorphosis is concurrent with settlement in winter flounder and appears as such in the IBM

The CO_2-treatment water was collected from a flow-through experimental CO_2-delivery system (Chambers et al. 2014). The system consists of a pre-treatment stage where source water from Sandy Hook Bay is filtered to 0.5 µm, sterilized with UV-lamps, and the pCO_2 lowered with a series of membrane contactors. The resulting water served as the source water for the experimental CO_2 treatments and was maintained aerated in head tanks using CO_2-stripped air. Each CO_2 (pH) experimental treatment level was created by counter-current diffusion of CO_2 gas at different concentrations into gravity fed columns of the source water. The CO_2 treatment water was delivered to tanks that were placed in water baths to achieve the temperature treatments in some of the experiments.

The concentrations of CO_2 used in the preliminary trials and the experiments (Table S1) are referenced as low, moderate, high, and very high (Experiment 1 only) pCO_2 water. The water of different CO_2 concentrations was delivered to one of four water baths (nominal temperatures of 4, 7, 10, and 13 °C with +/- 0.5 °C range) for rearing larvae (Experiment 2) or was transferred to walk-in temperature control rooms held at matching temperatures (Experiments 1 and 3). These temperatures are within the viable range for winter flounder embryos, larvae, and young juveniles. Carbonate chemistry of the treatment water was monitored continuously by pH probes. Following previous methods (Chambers et al. 2014), discrete water samples were used to validate pH with electrode and spectrophotometer and to quantify dissolved inorganic carbon via coulometer from which pCO_2 and other carbonate chemistry parameters were estimated using CO2SYS (Dickson et al. 2007).

S3.1. Experiment 1: Fertilization rate

Ripening adult winter flounder were collected by otter trawl from coastal waters in northern New Jersey on January 30, 2014 and transported to the NOAA facility. Captive fish were maintained in round tanks supplied with temperature-controlled local bay water (5˚C, 20 to 26 PSU, and pH 7.46 to 7.63) and held under ambient lighting. Spontaneous gonadal ripening allowed for controlled strip-spawning within two weeks of capture. Individual ripe females were transferred to a temperature-controlled room (4 °C) and a subset of their eggs was extruded by pressure into a 50-mL glass beaker that was then covered and placed on ice until eggs were used in the fertilization experiment. Milt was extruded by gently pressing each male near its urogenital pore, collected via glass transfer pipettes, and transferred to plastic centrifuge tubes, which were on ice. Gametes were generally used within 1 h of collection (maximum 5 h) but prior experience has shown gametes to be viable for up to 8 and 24 h for eggs and milt, respectively.

Two preliminary trials were run to ensure that fertilization could occur at all CO_2 × temperature treatment combinations, and all adult fish used in the fertilization experiment had viable gametes. Fertilization at all treatment combinations was confirmed by micro-pipetting a small drop of eggs (20 µl of unfertilized eggs containing approximately 60 eggs) from each female into 6-cm diameter plastic petri dishes. A small volume (10-µl) of milt, collected from three males and mixed immediately prior to use, was placed into 50 mL of treatment water to activate the sperm, then poured into the egg dish. Fertilization was scored within 24 h (details below). The quality of the gametes used from each parent used in preliminary trial 1 and in the full experiment (below) was also confirmed by using a dry fertilization technique. This dry method mixes gametes before flooding them with water to ensure a high density of milt and thus maximize the likelihood of successful fertilization. Two replicates dishes of each full-sibship (one female, one male) cross at each temperature were performed. Fertilization was scored within 24 h (details below). Gamete quality was confirmed for all parents used in the fertilization experiment.

For the fertilization rate experiments, each CO_2 x temperature treatment combination was evaluated using gametes from three to seven unique full-sibship crosses (milt from one male mixed with eggs from one female) with two replicate dishes per cross within each treatment combination. The fertilization protocol consisted of pipetting 20 µl of recently collected unfertilized eggs (~ 60 eggs) from one female into a 60-mm diameter plastic petri dish, and temporarily setting the dish aside. Milt from one male (5-µl volume) was added directly to 50 mL of CO_2 x temperature treatment water and slowly mixed for 10 s while simultaneously pouring 15 mL of treatment water over the set-aside eggs. The separate inundation of eggs and milt lasted 1 min after which 15 mL of the milt water was added to the egg petri dish then the dish swirled before briefly setting it aside for 1 min. After 1 min, the contents of the fertilization dish were gently poured onto a 600-µm nylon mesh that retained the eggs. Eggs were then rinsed with the low-pCO_2 water, transferred to a clean plastic petri dish holding 20 mL of low-pCO_2 water, and then set aside until scoring fertilization.

In all cased, eggs were scored within 24 h of gamete mixing by examination at 12-x magnification using a Leica dissecting microscope. Eggs were scored as either fertilized, unfertilized, or poor egg quality. Eggs of poor quality re opaque or irregularly shaped and are not candidates for successful fertilization regardless of the CO_2 x temperature treatment combination so they were not included in determining the proportion of total eggs fertilized under the various treatment conditions. Fertilization rate was calculated for each replicate of a cross within each treatment combination.

S3.2. Experiment 2: Length at metamorphosis

The parents of winter flounder early life stages used in experiment 2 were collected by otter trawl near Stellwagen Bank, Massachusetts. Fertilized eggs were received at the NOAA lab at 3 days post fertilization and groups of 250 eggs were distributed into egg baskets floated in 12-L tanks in each CO_2-×-temperature combination in the flow-through experimental CO_2-delivery system described above (Chambers et al. 2014). For this experiment low, moderate, and high CO_2 concentrations and two temperatures (10 and 13 °C) were used (Table S1), each present in duplicate. Upon hatching, larvae were moved from the egg basket into the 12-L tanks that had housed the basket. Larvae were fed enriched rotifers for the first three quarters of the larval period followed by co-feeding with larger zooplankton (enriched *Artemia*). Eye migration was used as the operative feature of metamorphosis and occurred 4 to 6 weeks after hatching with survival from ~ 50 to 70%, both responses varying with pCO_2 and temperature. Each individual was removed from the larval tank at metamorphosis (i.e., when the migrating eye reached the dorsal midline), anaesthetized, photographed at 6-X magnification for later image-based size determination, and then relocated to individual containers to be used in prey consumption trials (Experiment 3). Size at metamorphosis was measured by five morphometric characters but total length is used here.

S3.3. Experiment 3: Maximum prey consumption of recently settled juveniles

Determining maximum prey consumption used the recently settled juveniles from Experiment 2 and employed a predator-prey functional response approach (Holling 1959). One juvenile of known size and CO_2 x temperature history during the larval period was placed in a 9.5-cm diameter glass dish filled with 150 mL of UV-sterilized, 0.5-µm filtered seawater and fasted for 16 h in a 16 °C temperature-controlled room. The following day, a fixed number of prey (*Artemia*) drawn from a geometric series (2, 4, 8, 16, 32, 64, 128, or 256) was added to each container, which commenced at 22-h prey consumption trial. After 22 h, the flounder juvenile was removed, the surviving prey counted, and the prey number consumed determined by subtraction. Each prey density was replicated up to four times with any predator being used only once in the entire experiment. A Holling Type II prey saturation function was fit to the number of prey consumed vs number of prey offered (Hassell 1978). Maximum consumption rate for juvenile flounder as a function of larval CO_2 x temperature history was estimated as the asymptote of the Holling Type II prey saturation function.

Table S1. Summary of experiments on winter flounder early life-stages

Source	Life-stage	Treatment		Response	CO_2 effect
		pCO_2 (µatm) / pH	Temperature (°C)		
New Jersey	Gametes	498/8.0, 674/7.9, 1,275/7.7, 2,370/7.4	4, 7, 10, 13	Fertilization	Optimum fertilization at intermediate pH (see Fig. S1)
Massachusetts	Larvae	481/7.9, 860/7.8, 1,320/7.6	10, 13	Size at metamorphosis	Length reduced by ~2% in low pH treatments
Massachusetts	Larvae	481/7.9, 860/7.8, 1,320/7.6	10, 13	Maximum prey consumed by settled juveniles	Consumption reduced by ~20% in low pH treatments

S3.4. Data analysis and model implementation

Potential CO_2 effects on fertilization were defined using the same GAM analysis (of results from experiment 1) as for the calibrated model (Table S1, Supplement 2 Section S2.1.3.). The GAM predicted the logit-transformed fertilization success, or $\log\left(\frac{\text{fertilized ova}}{\text{unfertilized ova}}\right)$, as a function of temperature and smoothed pH and provided a good fit to the data (R^2=0.85, Figure S2). The predicted odds of fertilization were approximately 3 times and 1.5 times as high at the optimum CO_2 level (pH=7.624) as in the lowest CO_2 (pH=8.0) and highest CO_2 (pH=7.4) experimental treatments, respectively. Since the pH range experienced by benthic winter flounder gametes *in situ* is not well constrained, elevated CO_2 could result in either an increase or decrease in fertilization success. Consequently, we defined two potential CO_2 effects, each consistent with both the laboratory data and the assumptions of the calibrated model with no CO_2 effect (a_v =86.63% fertilization success at 0 °C with a temperature slope of b_v=-1.308% °C^{-1}). The increased fertilization effect (a_v=95.52%, b_v=-0.624% °C^{-1}) mimicked acidification from 8.0 to 7.624, while the decreased fertilization effect (a_v=80.07%, b_v=-1.571% °C^{-1}) mimicked acidification from 7.624 to 7.4. As with the calibrated model (Supplement 2 Section S2.1.3.) the values of parameters a_v and b_v were calculated by back-transforming GAM output from log-odds to raw fertilization success and then fitting linear approximations to the resulting curves ($R^2$0.99).

The CO_2 effect on size at settlement was based on unpublished measurements (experiment 2) of length at metamorphosis (eye migration past midline) and *ad libitum* prey consumption rate 2 days after metamorphosis, for winter flounder reared from eggs in high CO_2 treatments (pH=7.8 and 7.6) and controls (pH=7.9). A small reduction in length (~2%) and a much more dramatic reduction in consumption (~-20%) were observed. In context of the length-mass relationship implemented in the model, these effects were not consistent with each other. Individuals consuming 20% less food could not keep up in terms of growth and would quickly fall 2% behind in length. We reconciled this inconsistency by assuming that fish in elevated CO_2 treatments were also of lower condition (skinnier) at settlement, and that reduced consumption was indicative of lower mass as opposed to changed feeding behavior. Consequently, we modeled elevated CO_2 as reducing the size at settlement from 8 mm to 7.5 mm total length, corresponding to ~20% lower dry mass (350 µg versus 282 µg).

We added two generic CO_2 effects commonly demonstrated in laboratory experiments with other fish species. The generic effects were increased mortality at hatching, which is intended to represent deleterious malformations during embryonic development, and reduced or increased growth rate of feeding larvae. The sources used to derive these effects are discussed in Table 3 (main document).

Supplement 4. Robustness of results to temperature-dependent mortality and spawning timing.

To evaluate model sensitivity to two key processes assumed to be temperature-dependent in the IBM, the Reference and Severe simulations were repeated with temperature-independent versions. The temperature-dependent mortality rate was eliminated by assuming a $Q_m = 1$. The shift in spawning times due to warming temperatures was eliminated by fixing the spawning season to the dates calculated for the 1977-1986 (decade 1) period. Switching to temperature-independent mortality while maintaining the same balance of total and density-dependent mortality required re-tuning of the parameters for mortality rate at 10 °C ($a_m = 0.6038$) and density-dependent mortality ($d_m = 1.152e\text{-}11$). Fixing the timing of spawning to the decade prior to warming was implemented by substituting daily temperatures in that decade for those in subsequent decades until the day of spawning (e.g., the 1999 spawning season was determined by temperature during late 1978 to early 1979 instead of late 1998 to early 1999 temperatures).

Warming and elevated CO_2 conditions had similar effects under temperature-independent mortality and fixed timing of spawning as with the Reference simulation (Table S2). When the timing of spawning was fixed and not allowed to occur earlier in the year during later decades due to warming, similar effects of elevated of CO_2 on SSB were predicted. For example, the percentage change in SSB in decade 1 between Severe and Reference simulations was -18.8 for the original, -18.6 for temperature-independent, and -16.2 for fixed spawning. While elevated CO_2 had a much greater effect in decade 4, the effect was similar for all three conditions (-77.9 for original, -84.5 for temperature-independent, and -75.6 for fixed spawning).

Supplement 5. Additional model outputs.

Table S2. Percentage changes in averaged SSB by decade for additional Reference and Severe CO_2 simulations with the alternative assumptions of temperature-independent mortality and fixed timing of spawning. Percent change: ((Severe-Reference)/Reference *100)

Decade	Reported **in paper**		**Fixed spawning**		**Temperature-independent mortality**		**Percent change of Severe from Reference**		
	Reference	Severe	Reference	Severe	Reference	Severe	Reported in paper	Fixed spawning	Temperature-independent mortality
1	37.5	30.4	37.5	30.5	37.3	31.3	-18.8	-18.6	-16.2
2	38.0	16.8	37.2	15.8	37.1	18.0	-55.8	-57.6	-51.5
3	36.7	11.4	35.4	9.3	35.5	13.0	-69.0	-73.8	-63.4
4	26.3	5.8	24.3	3.7	28.2	6.9	-77.9	-84.5	-75.6

Table S3. Results of Retrospective simulation experiment with 10 elevated CO_2 effects simulations. These values were combined with the corresponding values from the Reference simulation in Table 6 (main document) to report percent changes in Table 8 (main document).

	Simulation									
	Decreased fertilization	**Increased fertilization**	**Smaller Settlement**	**Smaller and decreased**	**Smaller and increased**	**Malformed**	**Slower growth**	**Faster growth**	**Tradeoff**	**Severe**
	Duration (d)									
Embryo	18.0	18.0	18.0	18.0	18.0	17.9	18.0	17.9	18.0	18.0
Yolk-sac larva	7.5	7.5	7.5	7.5	7.5	7.5	7.5	7.5	7.5	7.5
Feeding larva	39.2	39.2	36.8	36.7	36.7	39.2	44.8	35.0	35.0	42.0
Settle to Dec 31	227.2	226.6	229.2	229.2	228.7	227.2	223.7	229.2	230	226.5
	Survival fraction									
Embryo	0.106	0.106	0.106	0106	0.106	0.080	0.106	0.106	0.080	0.080
Yolk-sac larva	0.428	0.429	0.428	0.428	0.429	0.429	0.428	0.429	0.429	0.429
Feeding larva **($x10^{-2}$)**	1.53	1.51	1.85	1.85	1.85	1.50	0.74	2.54	2.54	0.94
Settle to Dec 31 ($x10^{-3}$)	3.86	3.16	2.94	3.21	2.60	4.53	6.08	2.22	2.89	6.26
Body Mass on Dec 31 (g)	1.06	1.05	1.07	1.07	1.07	1.06	1.02	1.09	1.10	1.04
Body length on Dec 31 (mm)	86.02	85.85	86.29	86.31	86.14	86.01	84.90	86.64	86.89	85.45
Recruits per embryo ($x10^{-6}$)	2.639	2.148	2.439	2.665	2.160	2.314	2.035	2.546	2.488	2.007

Recruitment ($x10^6$)	55.6	63.4	60.6	57.5	64.4	48.0	29.0	73.2	66.3	20.3
SSB (kt)	33.1	36.7	35.4	33.9	37.2	29.5	20.4	41.3	38.1	16.1
Percent of age-3 mature	37.2	37.2	37.3	37.2	37.2	37.3	37.0	37.3	37.4	37.2
Embryos per age-3 ($x10^5$)	1.29	1.63	1.43	1.30	1.63	1.43	1.42	1.43	1.43	1.29

Table S4. Results for the Severe simulation of the Retrospective simulation experiment by decade. Reference results by decade are shown in Table 6 (main document). Overall averaged results (over all decades) for the Severe simulation are shown above.

Output	Stage	Decade			
		1	2	3	4
Spawning day (ordinal d)	Embryo	80.0	76.4	71.5	64.1
Duration (d)	Embryo	18.4	17.6	17.6	18.3
	Yolk-sac larva	7.4	7.4	7.5	7.6
	Feeding larva	41.1	41.5	42.0	43.1
	Settle to Dec 31	219.6	224.0	228.4	234.0
Survival fraction	Embryo	0.077	0.081	0.081	0.079
	Yolk-sac larva	0.430	0.431	0.428	0.426
	Feeding larva	0.0094	0.0095	0.0096	0.0092
	Settle to Dec 31	0.00634	0.00734	0.00627	0.00507
Body mass (g)	Dec 31	1.05	1.11	1.03	0.957
Body Length (mm)	Dec 31	85.72	87.30	85.44	83.35
Recruits per embryo ($x10^{-6}$)	Embryo to Dec 31	1.933	2.417	2.102	1.578
Recruitment ($x10^6$)	Dec 31	35.6	24.9	14.8	5.81
SSB (kt)	Adult	30.4	16.8	11.4	5.8
Percent of age-3 mature	Ova	37.9	38.5	36.8	35.4
Embryos per age 3 (10^5)	Embryo	1.33	1.36	1.27	1.20

Literature Cited

Black DE, Phelps DK, Lapan RL (1988) The effect of inherited contamination on egg and larval winter flounder, Pseudopleuronectes americanus. Mar Environ Res 25:45–62 doi:10.1016/0141-1136(88)90360-1

Brown JH, Gillooly JF, Allen AP, Savage VM, West GB (2004) Toward a metabolic theory of ecology. Ecology 85:1771–1789 doi:10.1890/03-9000

Buckley LJ (1980) Changes in RNA, DNA, and protein content during ontogenesis of the winter flounder Pseudopleuronectes americanus) and the effect of starvation. Fish Bull 77:703–708

Buckley LJ (1981) Biochemical changes during ontogenesis of cod (Gadus morhua L.) and winter flounder (Pseudopleuronectes americanus) larvae. Rapp P-V Reùn Cons Int Explor Mer 178:547–552

Buckley LJ (1982) Effects of temperature on growth and biochemical composition of larval winter flounder Pseudopleuronectes americanus. Mar Ecol Prog Ser 8:181–186 doi:10.3354/meps008181

Buckley LJ, Smigielski AS, Halavik TA, Laurence GC (1990) Effects of water temperature on size and biochemical composition of winter flounder Pseudopleuronectes americanus at hatching and feeding initiation. Fish Bull 88:419–428

Buckley LJ, Smigielski AS, Halavik TA, Caldarone EM, Burns BR, Laurence GC (1991a) Winter flounder Pseudopleuronectes americanus reproductive success. I. Among-location variability in size and survival of larvae reared in the laboratory. Mar Ecol Prog Ser 74:117–124 doi:10.3354/meps074117

Buckley LJ, Smigielski AS, Halavik TA, Caldarone EM, Burns BR, Laurence GC (1991b) Winter flounder Pseudopleuronectes americanus reproductive success. II. Effects of spawning time and female size on size, composition and viability of eggs and larvae. Mar Ecol Prog Ser 74:125–135 doi:10.3354/meps074125

Burton MP, Idler DR (1984) The reproductive cycle in winter flounder, Pseudopleuronectes americanus (Walbaum). Can J Zool 62:2563–2567 doi:10.1139/z84-374

Cetta CM, Capuzzo JM (1982) Physiological and biochemical aspects of embryonic and larval development of the winter flounder Pseudopleuronectes americanus. Mar Biol 71:327–337 doi:10.1007/BF00397049

Chambers RC, Candelmo AC, Habeck EA, Poach ME and others (2014) Effects of elevated CO_2 in the early life stages of summer flounder, *Paralichthys dentatus*, and potential consequences of ocean acidification. Biogeosciences 11:1613–1626 doi:10.5194/bg-11-1613-2014

DeCelles GR, Cadrin SX (2011) An interdisciplinary assessment of winter flounder (*Pseudopleuronectes americanus*) stock structure. J Northwest Atl Fish Sci 43:103–120 doi:10.2960/J.v43.m673

DeLong AK, Collie JS, Meise CJ, Powell JC (2001) Estimating growth and mortality of juvenile winter flounder, *Pseudopleuronectes americanus*, with a length-based model. Can J Fish Aquat Sci 58:2233–2246 doi:10.1139/f01-162

Dickson AG, Sabine CL, Christian JR, Bargeron CP (eds) (2007) Guide to best practices for ocean CO2 measurements. PICES special publication 3

Duan N (1983) Smearing estimate: a nonparametric retransformation method. J Am Stat Assoc 78:605–610 doi:10.1080/01621459.1983.10478017

Dunn RS, Tyler AV (1969) Aspects of the anatomy of the winter flounder ovary with hypotheses on oocyte maturation time. J Fish Res Board Can 26:1943–1947 doi:10.1139/f69-180

Frame DW (1973a) Biology of young winter flounder Pseudopleuronectes americanus (Walbaum); metabolism under simulated estuarine conditions. Trans Am Fish Soc 102:423–430 doi:10.1577/1548-8659(1973)102<423:BOYWFP2.0.CO;2

Frame DW (1973b) Conversion efficiency and survival of young winter flounder (Pseudopleuronectes americanus) under experimental conditions. Trans Am Fish Soc 102:614–617 doi:10.1577/1548-8659(1973)102<614:CEASOY2.0.CO;2

Hassell MP (1978) The dynamics of arthopod predator-prey systems. Princeton University Press.

Holling CS (1959) Some Characteristics of Simple Types of Predation and Parasitism1. Can Entomol 91:385–398 doi:10.4039/Ent91385-7

Houde ED, Zastrow CE (1993) Ecosystem-and taxon-specific dynamic and energetics properties of larval fish assemblages. Bull Mar Sci 53:290–335

Huebert KB, Peck MA (2014) A day in the life of fish larvae: modeling foraging and growth using Quirks. PLoS One 9:e98205 PubMed doi:10.1371/journal.pone.0098205

Huebner JD, Langton RW (1982) Rate of gastric evacuation for winter flounder, Pseudopleuronectes americanus. Can J Fish Aquat Sci 39:356–360 doi:10.1139/f82-049

Jearld A Jr, Sass SL, Davis MF (1993) Early growth, behavior, and otolith development of the winter flounder Pleuronectes americanus. Fish Bull 91:65–75

Kanstinger P, Beher J, Grenzdörffer G, Hammer C, Huebert KB, Stepputis D, Peck MA (2018) What is left? Macrophyte meadows and Atlantic herring (Clupea harengus) spawning sites in the Greifswalder Bodden, Baltic Sea. Estuar Coast Shelf Sci 201:72–81 doi:10.1016/j.ecss.2016.03.004

Keller AA, Klein-MacPhee G (2000) Impact of elevated temperature on the growth, survival, and trophic dynamics of winter flounder larvae: a mesocosm study. Can J Fish Aquat Sci 57:2382–2392 doi:10.1139/f00-217

Klein-MacPhee G (1978) Synopsis of biological data for the winter flounder Pseudopleuronectes americans (Walbaum). NOAA Tech Rep NMFS CIRC 414

Klein-Macphee G, Cardin JA, Berry WJ (1984) Effects of silver on eggs and larvae of the winter flounder. Trans Am Fish Soc 113:247–251 doi:10.1577/1548-8659(1984)113<247:EOSOEA2.0.CO;2

Laurence GC (1975) Laboratory growth and metabolism of the winter flounder Pseudopleuronectes americanus from hatching through metamorphosis at three temperatures. Mar Biol 32:223–229 doi:10.1007/BF00399202

Laurence GC (1977) A bioenergetic model for the analysis of feeding and survival potential of winter flounder, Pseudopleuronectes americanus, larvae during the period from hatching to metamorphosis. Fish Bull 75:529–546

Laurence GC (1979) Larval length-weight relations for 7 species of northwest Atlantic fishes reared in the laboratory. Fish Bull 76:890–895

Malloy KD, Targett TE (1991) Feeding, growth and survival of juvenile summer flounder Paralichthys dentatus: experimental analysis of the effects of temperature and salinity. Mar Ecol Prog Ser 72:213–223 doi:10.3354/meps072213

Malloy KD, Targett TE (1994) Effects of Ration Limitation and Low Temperature on Growth, Biochemical Condition, and Survival of Juvenile Summer Flounder from Two Atlantic Coast Nurseries. Trans Am Fish Soc 123:182–193 doi:10.1577/1548-8659(1994)123<0182:EORLAL2.3.CO;2

Manderson JP, Pessutti J, Shaheen P, Juanes F (2006) Dynamics of early juvenile winter flounder predation risk on a North West Atlantic estuarine nursery ground. Mar Ecol Prog Ser 328:249–265 doi:10.3354/meps328249

McBride RS, Wuenschel MJ, Nitschke P, Thornton G, King JR (2013) Latitudinal and stock-specific variation in size- and age-at-maturity of female winter flounder, Pseudopleuronectes americanus, as determined with gonad histology. J Sea Res 75:41–51 doi:10.1016/j.seares.2012.04.005

McCoy MW, Gillooly JF (2008) Predicting natural mortality rates of plants and animals. Ecol Lett 11:710–716 PubMed doi:10.1111/j.1461-0248.2008.01190.x

McElroy WD, Wuenschel MJ, Press YK, Towle EK, McBride RS (2013) Differences in female individual reproductive potential among three stocks of winter flounder, Pseudopleuronectes americanus. J Sea Res 75:52–61 doi:10.1016/j.seares.2012.05.018

Meng L, Gray C, Taplin B, Kupcha E (2000) Using winter flounder growth rates to assess habitat quality in Rhode Island's coastal lagoons. Mar Ecol Prog Ser 201:287–299 doi:10.3354/meps201287

Millstone Environmental Laboratory (2017) Winter flounder studies. In: Dominion Nuclear Connecticut, Inc. Annual report 2016. Monitoring the marine environment of Long Island Sound at Millstone Power Station, Waterford, Connecticut. Millstone Environmental Laboratory,Waterford, CT, p 111–144

Mulkana MS (1966) Habits of juvenile fishes in two Rhode Island estuaries. Gulf Res Rep 2:97–167

NEFSC (Northeast Fisheries Science Center) (2011) 52nd Northeast Regional Stock Assessment Workshop (52nd SAW) assessment summary report. NEFSC Ref Doc 11-11. Northeast Fisheries Science Center, Woods Hole, MA

Nelson DA, Miller JE, Rusanowsky D, Greig RA and others (1991) Comparative reproductive success of winter flounder in Long Island Sound: a three-year study (biology, biochemistry, and chemistry). Estuaries 14:318 doi:10.2307/1351666

NOAA National Estuarine Research Reserve System (NERRS) System-wide Monitoring Program. (2017) NERRS SWMP Water Quality Monitoring Data. www.nerrsdata.org (accessed February 24, 2017)

Pearcy WG (1962) Ecology of an estuarine population of winter flounder, *Pseudopleuronectes americanus* (Walbaum). Parts I–IV. Bull Bingham Oceanogr Collect 18(1):1–77

Pepin P (1991) Effect of temperature and size on development, mortality, and survival rates of the pelagic early life history stages of marine fish. Can J Fish Aquat Sci 48:503–518 doi:10.1139/f91-065

Press YK, McBride RS, Wuenschel MJ (2014) Time course of oocyte development in winter flounder *Pseudopleuronectes americanus* and spawning seasonality for the Gulf of Maine, Georges Bank and southern New England stocks: *pseudopleuronectes americanus* oogenesis. J Fish Biol 85:421–445 PubMed doi:10.1111/jfb.12431

Rogers CA (1976) Effects of temperature and salinity on the survival of winter flounder embryos. Fish Bull 74:52–58

Rose KA, Kimmerer WJ, Edwards KP, Bennett WA (2013) Individual-based modeling of delta smelt population dynamics in the upper San Francisco Estuary: I. model description and baseline results. Trans Am Fish Soc 142:1238–1259 doi:10.1080/00028487.2013.799518

Rose KA, Fiechter J, Curchitser EN, Hedstrom K and others (2015) Demonstration of a fully-coupled end-to-end model for small pelagic fish using sardine and anchovy in the California Current. Prog Oceanogr 138:348–380 doi:10.1016/j.pocean.2015.01.012

Scheffer M, Baveco JM, DeAngelis DL, Rose KA, van Nes EH (1995) Super-individuals a simple solution for modelling large populations on an individual basis. Ecol Modell 80:161–170 doi:10.1016/0304-3800(94)00055-M

Sogard S (1992) Variability in growth rates of juvenile fishes in different estuarine habitats. Mar Ecol Prog Ser 85:35–53 doi:10.3354/meps085035

Stierhoff K, Targett T, Miller K (2006) Ecophysiological responses of juvenile summer and winter flounder to hypoxia: experimental and modeling analyses of effects on estuarine nursery quality. Mar Ecol Prog Ser 325:255–266 doi:10.3354/meps325255

Taylor DL (2003) Size-dependent predation on post-settlement winter flounder Pseudopleuronectes americanus by sand shrimp Crangon septemspinosa. Mar Ecol Prog Ser Marine Ecology Progress Series 263:197–215 doi:10.3354/meps263197

Taylor DL, Danila DJ (2005) Predation on winter flounder (Pseudopleuronectes americanus) eggs by the sand shrimp (Crangon septemspinosa). Can J Fish Aquat Sci 62:1611–1625 doi:10.1139/f05-047

Thornton KW, Lessem AS (1978) A temperature algorithm for modifying biological rates. Trans Am Fish Soc 107:284–287 doi:10.1577/1548-8659(1978)107<284:ATAFMB2.0.CO;2

Tumbiolo ML, Downing JA (1994) An empirical model for the prediction of secondary production in marine benthic invertebrate populations. Mar Ecol Prog Ser 114:165–174 doi:10.3354/meps114165

Voyer RA, Morrison GE (1971) Factors affecting respiration rates of winter flounder (Pseudopleuronectes americanus). J Fish Res Bd Can 28:1907–1911 doi:10.1139/f71-287

Wigley SE, McBride HM, McHugh NJ (2003) Length-weight relationships for 74 fish species collected during NEFSC research vessel bottom trawl surveys, 1992-99. NOAA Tech Memo NMFS-NE-171

Wilber DH, Clarke DG, Gallo J, Alcoba CJ, Dilorenzo AM, Zappala SE (2013) Identification of winter flounder (Pseudopleuronectes americanus) estuarine spawning habitat and factors influencing egg and larval distributions. Estuaries Coasts 36:1304–1318 doi:10.1007/s12237-013-9642-z

Williams GC (1975) Viable embryogenesis of the winter flounder Pseudopleuronectes americanus from - 1.8° to 15°C. Mar Biol 33:71–74 doi:10.1007/BF00395003

Witherell DB, Burnett J (1993) Growth and maturation of winter flounder, Pleuronectes americanus, in Massachusetts. Fish Bull 91:816–820

Worobec MN (1984) Field estimates of the daily ration of winter flounder, Pseudopleuronectes americanus (Walbaum), in a southern New England salt pond. J Exp Mar Biol Ecol 77:183–196 doi:10.1016/0022-0981(84)90057-1